Evolution of three-dimensional correlations during the photoinduced melting of antiferromagnetic order in $La_{0.5}Sr_{1.5}MnO_4$

R. I. Tobey,[1,*] S. Wall,[2] M. Först,[3] H. Bromberger,[3] V. Khanna,[3,4,5] J. J. Turner,[6] W. Schlotter,[6] M. Trigo,[7] O. Krupin,[6,8] W. S. Lee,[9] Y.-D. Chuang,[10] R. Moore,[9] A. L. Cavalieri,[3] S. B. Wilkins,[1] H. Zheng,[11] J. F. Mitchell,[11] S. S. Dhesi,[4] A. Cavalleri,[3,5] and J. P. Hill[1]

[1]*Condensed Matter Physics and Materials Science Department, Brookhaven National Laboratory, Upton, New York 11973, USA*

[2]*Fritz-Haber Institute of the Max Planck Society, Berlin, Germany*

[3]*Max-Planck Department for Structural Dynamics, Center for Free Electron Laser Science, University of Hamburg, Germany*

[4]*Diamond Light Source, Chilton, Didcot, Oxfordshire OX11 0DE, United Kingdom*

[5]*Department of Physics, Clarendon Laboratory, Oxford University, United Kingdom*

[6]*Linac Coherent Light Source, SLAC National Accelerator Laboratory, Menlo Park, California 94025, USA*

[7]*PULSE Institute, SLAC National Accelerator Laboratory, Menlo Park, California 94025, USA*

[8]*European XFEL GmbH, Hamburg, Germany*

[9]*The Stanford Institute for Materials and Energy Sciences (SIMES), SLAC National Accelerator Laboratory, Menlo Park, California 94025, USA*

[10]*Advanced Light Source, Lawrence Berkeley National Laboratory, Berkeley, California 94720, USA*

[11]*Material Science Department, Argonne National Laboratory, Argonne, Illinois 60439, USA*

(Received 24 February 2012; revised manuscript received 16 July 2012; published 17 August 2012)

Using time-resolved resonant soft x-ray diffraction, we measure the evolution of the full three-dimensional scattering volume of the antiferromagnetic superlattice reflection in the single-layer manganite $La_{0.5}Sr_{1.5}MnO_4$ on femtosecond time scales following photoexcitation. We find that the in-plane correlations are unchanged as a metastable state is entered, however there are subtle changes in the *c*-axis correlations. We observe a transient shift of the scattering ellipsoid along $(00L)$ at very short times, and at longer time scales the short-range *c*-axis correlations are more robust than they are in equilibrium. Such results are not obtainable with any other techniques and hint at previously unresolved processes in the dynamics of photomelting in strongly correlated systems.

DOI: 10.1103/PhysRevB.86.064425 PACS number(s): 75.78.Jp, 78.47.D−, 71.27.+a

I. INTRODUCTION

Photoinduced dynamics in strongly correlated electron materials has garnered attention both for the insight it provides into the competing degrees of freedom underlying the various ground states of these systems, and for its potential technological applications. Due to the strong electronic correlations, laser-induced dynamics proceeds along strongly nonequilibrium pathways, evolves on ultrafast time scales, and can result in metastable states that persist for picoseconds or even nanoseconds. Examples of such photostimulated transitions in strongly correlated oxides include the photoinduced insulator-to-metal transition[1] and the vibrationally driven analog[2] in the manganites, and the switching of ferromagnetic domains in ferrites.[3] However, the microscopic mechanisms that drive these transitions remain hidden, in large part due to the complex interplay of multiple degrees of freedom such as lattice, charge, orbital, and spin that occurs in the ground and excited states.

Femtosecond short-wavelength probes, such as ultrafast x rays, enable the measurement of multiple degrees of freedom individually at distinct scattering wave vectors, and allow the tracking of their evolution in the time domain.[4–7] By monitoring the temporal evolution of each degree of freedom, one builds a map of how energy is transferred internally and which degrees of freedom are most strongly coupled. A crucial piece of this puzzle is to understand the length scales over which an order parameter is correlated and how these correlations evolve when the sample is driven out of equilibrium. This can only be done through measurement of time-resolved scattering. To date, however, no experiment has probed the temporal evolution of relevant correlations in three dimensions.

Using time-resolved resonant soft x-ray diffraction (RSXD), we reconstruct the full three-dimensional scattering volume of the (0.25, −0.25, 0.5) antiferromagnetic superlattice reflection in the strongly correlated oxide $La_{0.5}Sr_{1.5}MnO_4$(LSMO). We extract the correlation lengths and the ordering wave vector of magnetic ordering with femtosecond resolution along the three principal axes during a photoexcited electronic melting process. We find that the in-plane correlations are unchanged in this process, but we observe subtle changes in the *c*-axis correlations, specifically the emergence and recovery of a transient *c*-axis incommensurate antiferromagnetic ordering ∼1 ps after photoexcitation. As the system evolves into the metastable state, commensurate magnetic ordering is recovered, but the wings of the scattering ellipsoid indicate that short-range magnetic correlations along the *c* axis remain suppressed.

II. EXPERIMENTAL

The material chosen for this study, $La_{0.5}Sr_{1.5}MnO_4$, is the exemplar charge, orbital, and spin ordered manganite.[8] Neutron,[9–11] hard x-ray,[10] and soft x-ray[12–15] scattering techniques have been employed to study the static properties of long-range charge, orbital, and spin ordering in this material. In the present study, we focus on the magnetic degree of freedom, which can be probed at a wave vector of

(0.25, −0.25, 0.5) below the Néel temperature, $T_N = 120$ K. The sample used in our experiments was prepared using the floating zone technique, and subsequently cut and polished with the surface normal along $(1\bar{1}0)$. It was mounted on a five-circle diffractometer in the soft x-ray (SXR) hutch of the Linac Coherent Light Source (LCLS)[16] and cooled to 25 K. Soft x rays, resonant with the Mn L_3 edge ($E = 642$ eV, $\Delta E = 1.5$ eV), were focused to a spot of 250 μm diameter on the sample. This energy was chosen to maximize the magnetic scattering intensity.[12–15] The pump beam (1.5 eV) and x rays were brought together upstream of the diffractometer and collinearly propagated to the sample position. The pump beam spot size was 400 μm × 600 μm, ensuring a uniform excitation of the probed region. Both pump and probe impinge on the sample at a near normal angle of incidence with π-polarization. Spatial and temporal overlap at the sample position was verified by using a small removable aperture and a photoionization antenna, respectively. The arrival time of the pump beam relative to the x rays was varied with a mechanical delay stage. Scattered x rays were detected with an in-vacuum CCD camera capable of recording individual shots of the free electron laser (FEL).[17] The images are background corrected using a dark image taken in the absence of the FEL beam and binned according to the scattering angles and time delay between pump and probe. Figure 1(a) shows a representative, background corrected, "raw" CCD image for the antiferromagnetic reflection (0.25, −0.25, 0.5). This image is comprised of roughly 300 individual FEL shots, accumulated over approximately 5 s with the accelerator operating at 60 Hz.

Reconstruction of the 3D reciprocal space volume is aided by using this pixelated detector, as shown in the scattering schematic in Fig. 1(b). Importantly, each pixel of the detector corresponds to a distinct position in reciprocal space (H K L), providing a means for parallel acquisition of many (H K L) points at once. Transformation of each image into reciprocal space is achieved by applying the appropriate UB matrix[18] to the scattering geometry. Through a combined motion of the sample angle, θ, and detector angle, 2θ, an ensemble of images is acquired as the camera is moved through the scattering volume. The full 3D reciprocal space representation of the scattering volume is then reconstructed from these images. Since each volume element in reciprocal space is populated by a large number of CCD pixels, the average scattering amplitude and standard deviations are readily assessed. (The package used for processing CCD images into reciprocal space maps was developed by Sven Partzsch and Stuart Wilkins and implemented in PYTHON within the PYSPEC package. More information can be obtained from S. Wilkins directly at swilkins@bnl.gov.)

III. RESULTS AND DISCUSSION

The outcome of this transformation is shown in Fig. 2, in which slices through the reconstructed 3D volume are presented for the case of no laser excitation. Data along the L direction are limited by the maximum detector angle of 150° and thus a measurement of just over half the scattering volume is possible in this direction. However, the significant

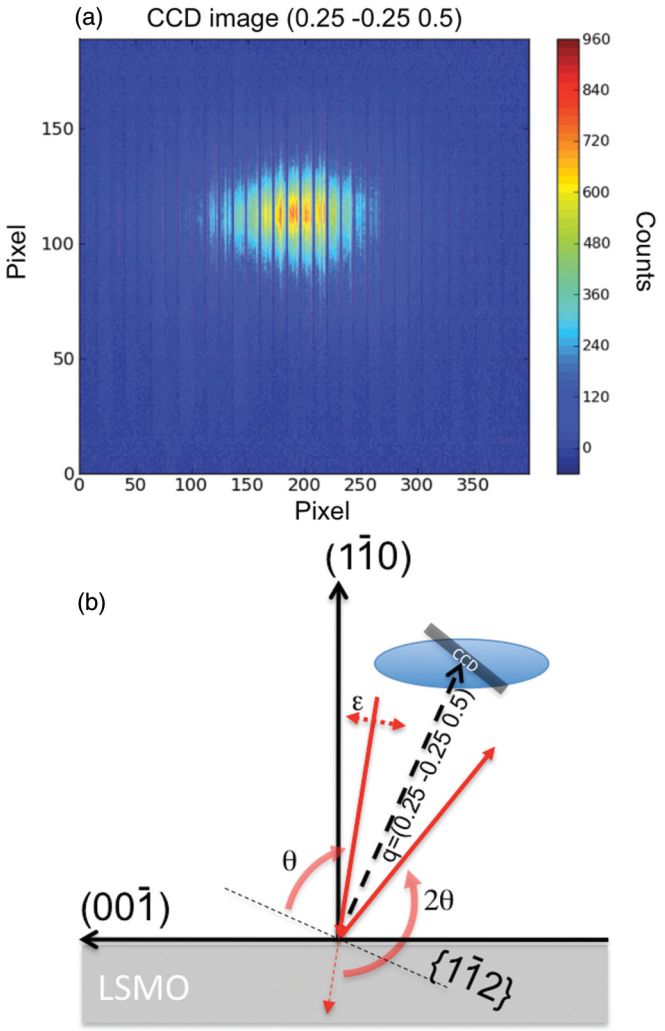

FIG. 1. (Color online) Representative CCD image of the antiferromagnetic superlattice reflection (0.25, −0.25, 0.5) (top). Readout registers are placed every ten pixel columns for enhanced acquisition rates and appear as black stripes. Schematic of the scattering geometry used (bottom). The CCD camera is shown cutting through the scattering volume, which is elongated along (0 0 1) due to poor c-axis correlations. Through a combined motion of sample and detector angles, the CCD samples the entire scattering volume.

elongation along the L direction due to the extremely short c-axis correlation length[10] is clearly visible. In the HK plane, an elongation along the $(1\bar{1}0)$ surface normal direction is seen. This is attributed to the finite penetration depth of the x rays. Also included in Fig. 2 are line cuts through the maximum in the scattering volume along the three principal directions in reciprocal space and corresponding squared Lorentzian fits. Correlation lengths, as measured by $\frac{1}{\text{HWHM}}$ (where HWHM denotes half-width at half-maximum) of the fitted line shapes, of $\xi_a = \xi_b = 540 \pm 10$ Å and $\xi_c = 20 \pm 5$ Å, are in good agreement with published results.[10]

We now discuss the temporal evolution of the scattering volume. Figure 3(a) shows normalized (0.25, −0.25, L) line cuts through the reconstructed scattering volumes for three time delays: (i) laser blocked, defined as pre-T_0; (ii) 1.3 ps after laser excitation; and (iii) 9 ps after laser excitation. The data are

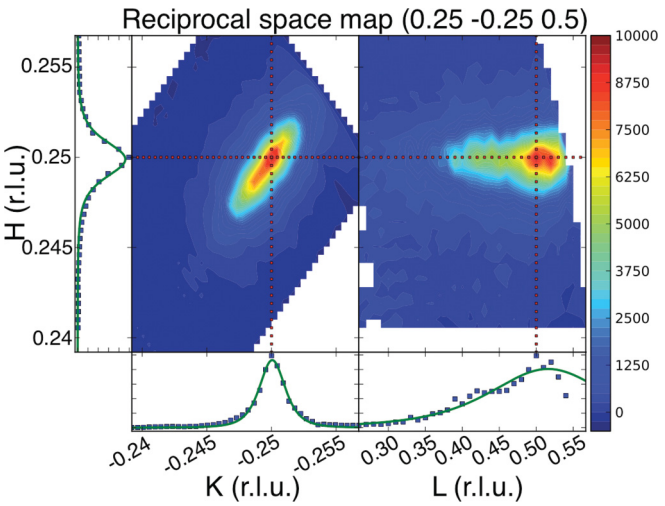

FIG. 2. (Color online) Slices through the maximum of the scattering volume in the HK and HL planes without laser excitation. Note the significantly expanded L-axis scale. Solid lines are the result of Lorentzian squared fits to the data.

averaged over a small region around $K = -0.25$ r.l.u. ($\delta k = 0.002\,75$). It is here that we catch a glimpse of the nontrivial dynamics at play. At the earliest time delay (1.3 ps), we observe a shift in the peak position along L of about 5% from $L = 0.5$ to 0.47 r.l.u. Subsequently, for the later time delay (9 ps), the peak maximum has shifted back to its original position

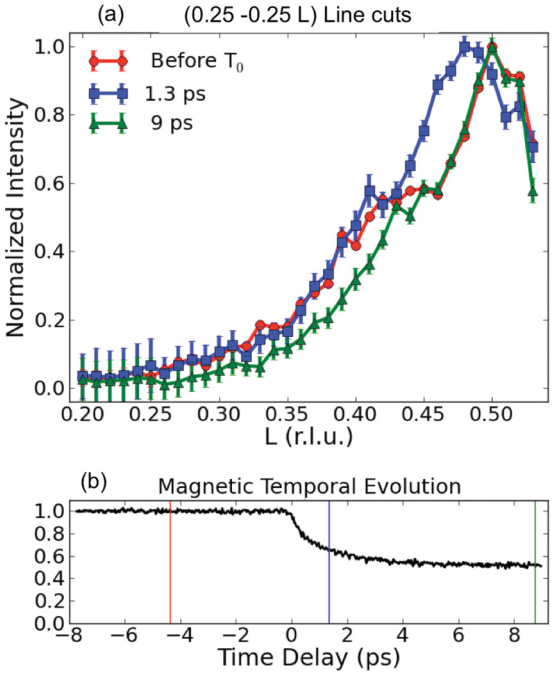

FIG. 3. (Color online) Line cuts (0.25, −0.25, L) for the three time delays (top), averaged over $\delta k = 0.002\,75$. The scattering volume shows a shift in scattering intensity 1.3 ps after excitation (blue). Recovery to the unpumped position (red) is seen by 9 ps time delay (green). The temporal evolution of the single CCD image (bottom) shows the onset of a long lived magnetic state, indicated by reduced scattering after T_0. Vertical lines show the temporal positions of the three scattering volume reconstructions.

and exhibits a reduction in scattering intensity in the wings, which appears as a prominent decrease from the unperturbed scattering between $0.3 < L < 0.45$. On these same time scales, a much smaller shift of 0.5% is also seen along the $(1\bar{1}0)$ direction (data not shown). This latter, small shift can readily be attributed to a thermoacoustic response due to the excitation. However, this cannot explain the dynamics along the c axis, which lies in the scattering plane, and therefore experiences uniform laser excitation.

To further emphasize the temporal aspects of the shift at 1.3 ps, Fig. 3(b) shows the evolution of a single slice through reciprocal space, obtained from the temporal evolution of a single "real space" CCD image [Fig. 1(a)]. The evolution of this single CCD image provides a means to quickly characterize the various temporal regimes of the photoexcited dynamics. We can identify two distinct temporal regimes, the first at early time delays where the scattering intensity is falling rapidly, and the second where the scattering intensity is constant and persists at this reduced scattering amplitude for greater than 160 ps, the limit of the scan range (see, e.g., Ref. 4). Crucially, we see that the time delay for which we see the shift (i.e., 1.3 ps) occurs during the first such period. Conversely, the 9 ps data, for which the peak has shifted back to its original position, correspond to the regime when the dynamics has reached this long-lived state (i.e., the metastable state).

We also study the evolution of the scattering ellipsoid along the H and K directions. In Fig. 4, we plot line cuts taken in the K direction for two different L values, specifically $L = 0.5$ and 0.4 r.l.u., for pre-T_0 and at 9 ps delay (at a constant $H = 0.25$ r.l.u.). The data sets have been normalized to have a unit peak intensity at (0.25, −0.25, 0.5) to facilitate comparison. If the line shape was unchanged when photoexcited, then both sets of curves would fall on top of one another. This is the case for $L = 0.5$. However, we see that away from the peak at $L = 0.4$ r.l.u., the intensity has fallen further at 9 ps than it has in the pre-T_0 data. In contrast, the in-plane line shapes are unchanged following photoexcitation. This is direct evidence that the in-plane correlations are unchanged, and that the c-axis

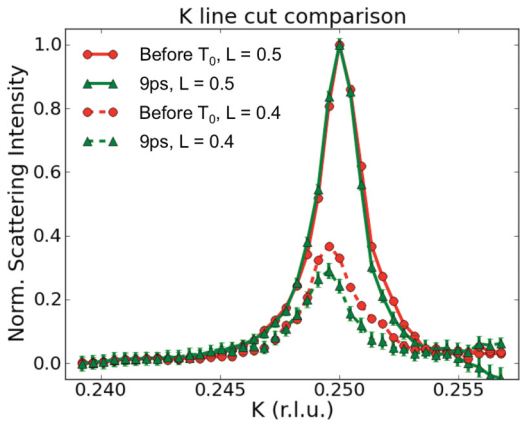

FIG. 4. (Color online) K line cut comparison at $L = 0.5$ and 0.4 r.l.u., taken at $H = 0.25$ r.l.u. When normalized to the value at $L = 0.5$, the intensity in the wings of the scattering ellipsoid, $L = 0.4$, is reduced in the transient state (9 ps) as compared to the equilibrium value (before T_0).

correlations in this metastable state do not decay with distance in the same way as they do in the equilibrium state. Specifically, we find that the tails of the scattering, at large δL from the peak, are weaker at 9 ps than they are at equilibrium. This, in turn, implies that spatial modulations on shorter length scales decay more slowly with distance in the transient state, while the long period, large length scale behavior is unchanged.

One possible explanation for the observed dynamics is of a photoinduced tendency toward magnetic incommensurability. It is not unexpected to observe modifications in the magnetic structure under ultrafast optical excitation. Photoexcitation in related materials has been proposed to dynamically modify the nearest-neighbor exchange interaction[19] driving changes in magnetic structure. In a related doped manganite, a photoinduced insulator-to-ferromagnet transition has been transiently induced[20] and measured using magneto-optics. The shift we observe in L implies a transient incommensurate modulation along the c axis. Indeed, such incommensurate phases are not uncommon at equilibrium in the manganites, where in-plane incommensurate phases are present in $La_{1-x}Sr_{1+x}MnO_4$ beyond $x = 0.5$ (Ref. 21) and in the related compound $Pr_{1-x}Ca_{1+x}MnO_4$ below $x = 0.5$.[22] For stoichiometric compounds, they are believed to arise from the competition between ferromagnetic double exchange and antiferromagnetic superexchange.[23] Therefore, it does not seem unreasonable to speculate that the photoexcitation of hot electrons into the unoccupied, out-of-plane e_g orbitals disturbs this balance and drives the transient incommensurability. However, we note that it is not possible to confirm such incommensurability without also observing a structural Bragg peak, which is not possible at these x-ray energies.

With regard to the changes observed in the tails, one possible explanation could be that optical excitation preferentially acts on one magnetic length scale more efficiently than another. We note the existence of a shoulder present in the equilibrium scattering peak, and its absence in the metastable state. This scattering may arise from regions of the sample with a shorter correlation length, perhaps driven by stacking faults, for example, which gives rise to a broader component to the scattering which appears here as something of a shoulder. The optical pump may preferentially melt (perhaps even thermally) the correlated patches with the shortest length scales, resulting in the loss of scattering intensity observed in the metastable state.

At present, we cannot confirm either of these two scenarios, and merely offer them as possibilities that will require further experiments to explore. In searching for an explanation of these data, we note that while fast structural modifications have been seen in similar compounds using femtosecond hard x-ray diffraction,[24] we cannot reconcile the observed shift and subsequent recovery of the peak position with such a long-lived structural state, and we expect that the changes observed in the magnetic scattering are not structurally driven.

IV. CONCLUSION

To summarize, we have used time-resolved resonant soft x-ray diffraction and a CCD camera to reconstruct the 3D scattering volume of the magnetic superlattice reflection (0.25, −0.25, 0.5) in $La_{0.5}Sr_{1.5}MnO_4$ during an ultrafast electronic melting process. This provides a unique, detailed view of the correlations during the photomelting process. We find that following photoexcitation, the order parameter is reduced, as measured by the integrated intensity of the scattering ellipsoid, but the average in-plane correlation lengths, as measured by $\frac{1}{\mathrm{HWHM}}$ of the scattering, are unchanged for all time delays measured. Additionally, we find changes to the out-of-plane real-space correlations. At the shortest delays, the scattering shifts to lower L values, recovering as the sample enters the metastable state. In the metastable state, the wings of the scattering ellipsoid are suppressed. These dynamics remain hidden when a single slice through reciprocal space is recorded. The data presented offer an intriguing glimpse into the dynamics of the magnetic degree of freedom in a correlated electron system driven out of equilibrium. With appropriate sample selection, orbital, magnetic, and structural modifications should elucidate any uncertainty in ascribing the observed shift to incommensurability. Future experiments will focus on reconstructing the scattering volumes of the orbital degree of freedom in order to correlate the observed magnetic behavior with changes in orbital ordering. Implementing our technique with soft x-ray free electron lasers allows the measurement of structural, charge, orbital, and spin correlation length scales in reciprocal-space and paves the way to accessing real-space dynamics on fundamental time and length scales.

ACKNOWLEDGMENTS

Work performed at BNL was supported by the US Department of Energy, Division of Materials Science, under Contract No. DE-AC02-98CH10886. S.W. acknowledges support from the Alexander Von Humboldt Foundation. Work performed at CFEL was funded by the Max Planck Research Group for Structural Dynamics at the University of Hamburg. Work at Argonne was supported by the US Department of Energy, Office of Science under Contract No. DE-AC02-06CH11357. Portions of this research were carried out on the SXR Instrument at the Linac Coherent Light Source (LCLS), a division of SLAC National Accelerator Laboratory and an Office of Science user facility operated by Stanford University for the US Department of Energy. The SXR Instrument is funded by a consortium whose membership includes the LCLS, Stanford University through the Stanford Institute for Materials Energy Sciences (SIMES), Lawrence Berkeley National Laboratory (LBNL), University of Hamburg through the BMBF priority program FSP 301, and the Center for Free Electron Laser Science (CFEL).

*Present address: Zernike Institute for Advanced Materials, University of Groningen, Groningen, The Netherlands; r.i.tobey@rug.nl

[1] K. Miyano, T. Tanaka, Y. Tomioka, and Y. Tokura, Phys. Rev. Lett. **78**, 4257 (1997).

[2] M. Rini, R. I. Tobey, N. Dean, J. Itatani, Y. Tomioka, Y. Tokura, R. W. Schoenlein, and A. Cavalleri, Nature (London) **449**, 72 (2007).

[3] A. V. Kimel, A. Kirilyuk, P. A. Usachev, R. V. Pisarev, A. M. Balbashov, and T. Rasing, Nature (London) **435**, 655 (2005).

[4]H. Ehrke, R. I. Tobey, S. Wall, S. A. Cavill, M. Foerst, V. Khanna, T. Garl, N. Stojanovic, D. Prabhakaran, A. T. Boothroyd *et al.*, Phys. Rev. Lett. **106**, 217401 (2011).

[5]N. Pontius, T. Kachel, C. Schuessler-Langeheine, W. F. Schlotter, M. Beye, F. Sorgenfrei, C. F. Chang, A. Foehlisch, W. Wurth, P. Metcalf *et al.*, Appl. Phys. Lett. **98**, 182504 (2011).

[6]K. Holldack, N. Pontius, E. Schierle, T. Kachel, V. Soltwisch, R. Mitzner, T. Quast, G. Springholz, and E. Weschke, Appl. Phys. Lett. **97**, 062502 (2010).

[7]M. Först, R. I. Tobey, S. Wall, H. Bromberger, V. Khanna, A. L. Cavalieri, Y. D. Chuang, W. S. Lee, R. Moore, W. F. Schlotter, J. J. Turner, O. Krupin, M. Trigo, H. Zheng, J. F. Mitchell, S. S. Dhesi, J. P. Hill, and A. Cavalleri, Phys. Rev. B **84**, 241104(R) (2011).

[8]Y. Moritomo, Y. Tomioka, A. Asamitsu, Y. Tokura, and Y. Matsui, Phys. Rev. B **51**, 3297 (1995).

[9]B. J. Sternlieb, J. P. Hill, U. C. Wildgruber, G. M. Luke, B. Nachumi, Y. Moritomo, and Y. Tokura, Phys. Rev. Lett. **76**, 2169 (1996).

[10]S. Larochelle, A. Mehta, L. Lu, P. K. Mang, O. P. Vajk, N. Kaneko, J. W. Lynn, L. Zhou, and M. Greven, Phys. Rev. B **71**, 024435 (2005).

[11]E. P. Houwman, G. Maris, G. M. DeLuca, N. Niermann, G. Rijnders, D. H. A. Blank, and S. Speller, Phys. Rev. B **77**, 184412 (2008).

[12]S. B. Wilkins, P. D. Spencer, P. D. Hatton, S. P. Collins, M. D. Roper, D. Prabhakaran, and A. T. Boothroyd, Phys. Rev. Lett. **91**, 167205 (2003).

[13]S. S. Dhesi, A. Mirone, C. De Nadai, P. Ohresser, P. Bencok, N. B. Brookes, P. Reutler, A. Revcolevschi, A. Tagliaferri, O. Toulemonde *et al.*, Phys. Rev. Lett. **92**, 056403 (2004).

[14]U. Staub, V. Scagnoli, A. M. Mulders, K. Katsumata, Z. Honda, H. Grimmer, M. Horisberger, and J. M. Tonnerre, Phys. Rev. B **71**, 214421 (2005).

[15]S. B. Wilkins, N. Stojic, T. A. W. Beale, N. Binggeli, C. W. M. Castleton, P. Bencok, D. Prabhakaran, A. T. Boothroyd, P. D. Hatton, and M. Altarelli, Phys. Rev. B **71**, 245102 (2005).

[16]P. Emma, R. Akre, J. Arthur, R. Bionta, C. Bostedt, J. Bozek, A. Brachmann, P. Bucksbaum, R. Coffee, F. J. Decker *et al.*, Nat. Photon. **4**, 641 (2010).

[17]D. Doering, Y. D. Chuang, N. Andresen, K. Chow, D. Contarato, C. Cummings, E. Domning, J. Joseph, J. S. Pepper, B. Smith *et al.*, Rev. Sci. Instrum. **82**, 073303 (2011).

[18]M. Lohmeier and E. Vlieg, J. Appl. Crystallogr. **26**, 706 (1993).

[19]S. Wall, D. Prabhakaran, A. T. Boothroyd, and A. Cavalleri, Phys. Rev. Lett. **103**, 097402 (2009).

[20]M. Matsubara, Y. Okimoto, T. Ogasawara, Y. Tomioka, H. Okamoto, and Y. Tokura, Phys. Rev. Lett. **99**, 207401 (2007).

[21]H. Ulbrich, D. Senff, P. Steffens, O. J. Schumann, Y. Sidis, P. Reutler, A. Revcolevschi, and M. Braden, Phys. Rev. Lett. **106**, 157201 (2011).

[22]F. Ye, S. Chi, J. A. Fernandez-Baca, A. Moreo, E. Dagotto, J. W. Lynn, R. Mathieu, Y. Kaneko, Y. Tokura, and P. Dai, Phys. Rev. Lett. **103**, 167202 (2009).

[23]J. Salafranca and L. Brey, Phys. Rev. B **73**, 024422 (2006).

[24]P. Beaud, S. L. Johnson, E. Vorobeva, U. Staub, R. A. De Souza, C. J. Milne, Q. X. Jia, and G. Ingold, Phys. Rev. Lett. **103**, 155702 (2009).